*Smart Structures and Systems, Vol. 8, No. 4 (2011) 413-431*
DOI: http://dx.doi.org/10.12989/sss.2011.8.4.413


# Exact solutions of the piezoelectric transducer under multi loads

Zhang Taotao*[1] and Shi Zhifei[2]

[1]*School of Transportation Science and Engineering, Beihang University, Beijing, 100191, P. R. China*
[2]*School of Civil Engineering, Beijing Jiaotong University, Beijing, 100044, P. R. China*

*(Received December 30, 2010, Revised July 13, Accepted August 6, 2011)*

**Abstract.** Under the external shearing stress, the external radial stress and the electric potential simultaneously, the piezoelectric hollow cylinder transducer is studied. With the Airy stress function method, the analytical solutions of this transducer are obtained based on the theory of piezo-elasticity. The solutions are compared with the finite element results of Ansys and a good agreement is found. Inherent properties of this piezoelectric cylinder transducer are presented and discussed. It is very helpful for the design of the bearing controllers.

**Keywords:** piezoelectric material; transducer; cylinder; multi-layer; shearing stress; radial stress.

## 1. Introduction

The discovery of the piezoelectric effect in 1880 have enabled wide application of the piezoelectric composites in the design of adaptive or smart structures, including aeronautical structures, automotive structures, miniature positioning devices and so on (Bboudi 1991, Muralt *et al*. 1986, Hagood and Von 1991, Rao and Sunar 1994, Loewy 1997, Yoon and Washington 1998). Multi-morph piezoelectric actuator was investigated and its behavior was predicted (Hauke *et al.* 2000). A micro multi-layered piezoelectric actuator containing a stack of piezoelectric crystals in a thin-layered compact structure was also proposed and its suitability as a stimulator in middle ear hearing implants was evaluated (Wang *et al.* 2002) and is capable of predicting the stress field and out-of-plane displacement of laminated piezoelectric layers. By using the solid element, the actuation performance of a multi-layered piezoceramic composite actuator was analyzed (Lee *et al*. 2002). A modified classical lamination theory (CLT) was developed to account for the piezoelectric coupling terms under applied electric field (Almajid *et al.* 2001). As opposed to traditional investigations based on the elementary theory of elasticity, one of the author (Shi) and his group have found the exact solutions of the piezoelectric composite cantilevers by introducing the recurrence techniques (Shi *et al.* 2006), as well as the exact solutions for a kind of functionally gradient piezo-thermo-elastic cantilever under certain coupled loads (Chen and Shi 2005). Furthermore, we studied the bending behavior of several piezoelectric curved actuators, including bi-morph actuators, functionally gradient actuators and 2-2 multi-layered actuators (Shi 2005, Zhang and Shi 2006, Zhang and Shi 2007). Recently, the analytical

*Corresponding Author, Dr., E-mail: zhangtt@buaa.edu.cn

solutions of two kinds of actuators, one is the expansion actuator and the other is the contraction actuator, were obtained based on the theory of piezo-elasticity (Han and Shi 2008). Actuators were under the external potential.

Among various symmetric and antisymmetric structures which play important roles in engineering, cylindrical structures received extensive attentions, such as the elastic cylinders (Olesiak and Pyryev Yu 1995, Xiang 2006) piezoelectric tubes (Ting 1999, Chen *et al.* 2000), hollow piezoelectric sphere/cylinder (Ding *et al.* 2003, Hou *et al.* 2003), piezo-thermo-elastic cylindrical panel (Sharma *et al*. 2004), antisymmetric laminated plates (Aldraihem and Khdeir 2006) and so on. A power series method was proposed for the solution of the static equilibrium equations of an axisymmetric composite cylinder under loadings due to surface mounted or embedded piezoelectric laminae (Mitchell and Reddy 1995). An exact solution of finitely long, simply supported, orthotropic, functionally graded piezoelectric, cylindrical shell was obtained by separation of variables under pressure and electrostatic excitation (Sedighi and Shakeri 2009). A mechanical impedance approach was employed for dynamically modeling distributed PZT actuator-driven thin cylindrical shells (Zhou *et al.* 1994). And new actuating method using piezoelectric (PZT) impact force coupled with differential pressure for the pneumatic positioning device was also reported (Liu and Higuchi 2001, Liu and Jiang 2007). However, investigations on the analytical solutions of piezoelectric composites under shearing load in the mechanic and electric field have not been found in the literatures.

The present paper is to study the properties of the piezoelectric hollow cylinder transducer under the external shearing stress, the external radial stress and the external potential simultaneously. That is to say this transducer can be treated as both sensors and actuators. When the external potential is not supplied, this transducer becomes a sensor; otherwise, this transducer can be treated as an actuator. Furthermore, this paper takes the external shearing stress into account and the shearing deformation of the actuators can be considered, which is very helpful for the design of the bearing controllers. The remainder of this paper is organized as follows. In Section 2, we listed the basic equations which will be utilized in Section 3. With the Airy stress function method, the analytical solutions of this transducer are obtained based on the theory of piezo-elasticity (Section 3). The solutions are then found to be well consistent with the finite element results of Ansys (Section 4). Furthermore, the inherent properties of this transducer are discussed and the conclusions are given in Section 5.

## 2. Basic equations

The interaction of expansion transducer and the target to be controlled can be simulated by Fig. 1(a). This transducer consists of two elastic layers (#1 and #2) and one piezoelectric layer. A gap with the size $\delta$ is between the actuator's elastic layer and the target layer (#3) to be controlled. The thickness of each layer can be determined by the radii $R_0$, $R_1$, $R_2$, $R_3$, $R_4$, and $R_5$. Between the inner and outer surfaces of the piezoelectric layer, an external electrical potential $V_0$ is applied. Besides, the shearing stress $\tau_0$ and the radial stress $\sigma_0$ are acting on the outer surface of the elastic layer 3. Let $\tau_0 = \mu\sigma_0$, $\mu$ is the friction coefficient of the elastic layer 3.

With the polar coordinate system ($r$-$O$-$\theta$), symbols $S_r$, $S_\theta$, $S_{r\theta}$ denote the strain, $T_r$, $T_\theta$, $T_{r\theta}$ the stress, $E_r$, $E_\theta$ the electric field, $D_r$ the induction along the direction indicated by their respective subscripts. Without consideration of body force and body charge, the constitutive equations for transversely isotropic elastic materials and piezoelectric materials undergoing a plane deformation

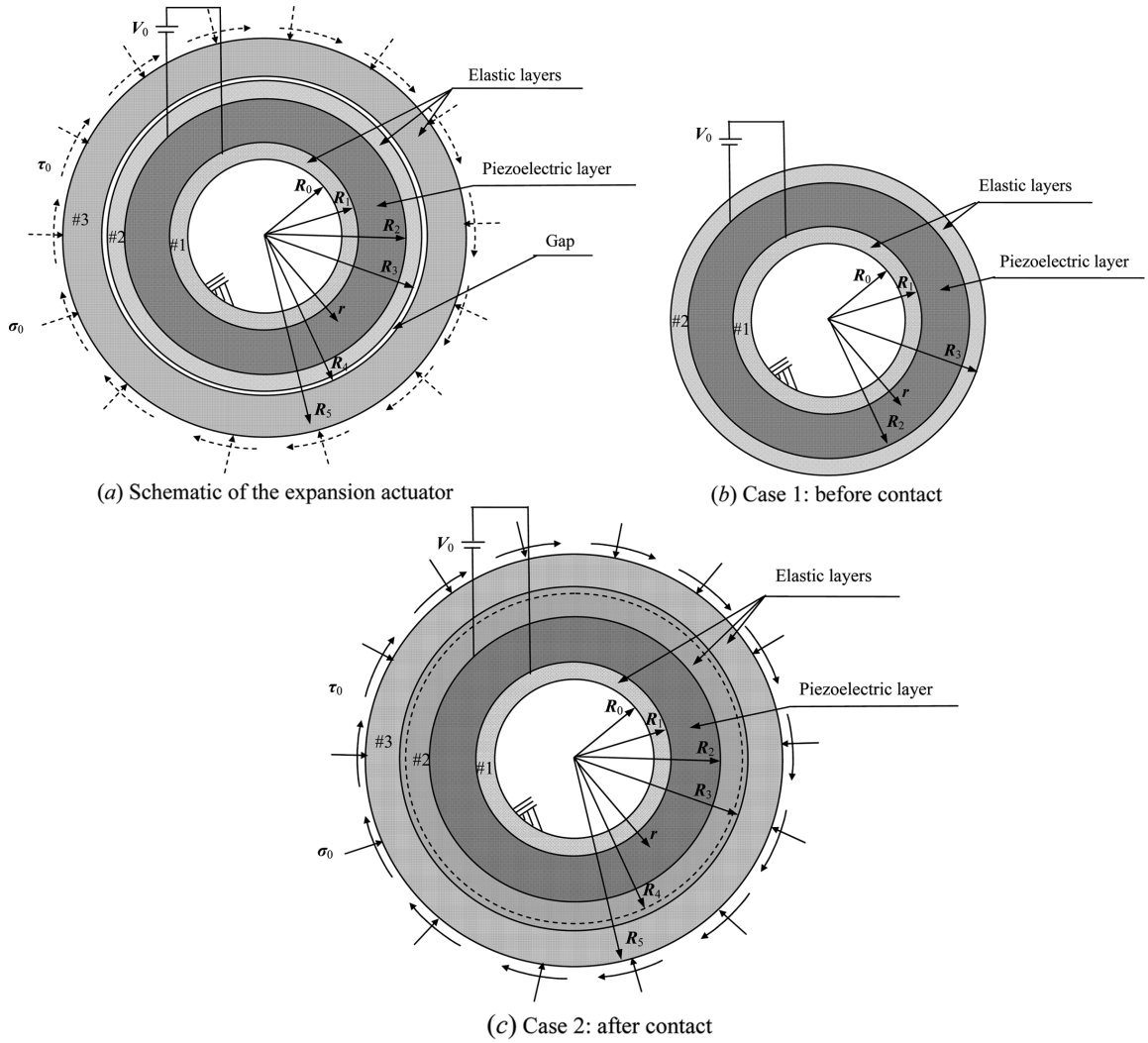


Fig. 1 Schematic of the expansion actuator (model A)

can be written as follows according to the IEEE standard

$$\begin{cases} S_\theta = S_{11E}T_\theta + S_{13E}T_r \\ S_r = S_{13E}T_\theta + S_{33E}T_r \\ S_{r\theta} = S_{44E}T_{r\theta} \end{cases} \quad \text{(for elastic layer 1, 2, 3)} \tag{1a}$$

$$\begin{cases} S_\theta = S_{11P}^D T_\theta + S_{13P}^D T_r + g_{31}D_r \\ S_r = S_{13P}^D T_\theta + S_{33P}^D T_r + g_{33}D_r \\ S_{r\theta} = S_{44P}^D T_{r\theta} + g_{15}D_\theta \\ E_\theta = -g_{15}T_{r\theta} + \beta_{11}^{\mathrm{T}} D_\theta \\ E_r = -g_{31}T_\theta - g_{33}T_r + \beta_{33}^{\mathrm{T}} D_r \end{cases} \quad \text{(for piezoelectric layer)} \tag{1b}$$

where $S_{klE}$ and $S_{klP}^{D}$ ($k = 1,4$; $l = 1,3,4$) are the coefficients of the effective elastic compliance for the elastic layers and piezoelectric layers, respectively. The superscript D denotes $S_{klP}^{D}$ is measured under the open circuit. The subscript "$E$" and "$P$" denote the corresponding variables and parameters in the elastic layers and piezoelectric layer, respectively. The coefficients of the piezoelectric and dielectric impermeability for the piezoelectric layers are denoted by $g_{31}$, $g_{33}$, $g_{15}$ and $\beta_{11}^{T}$, $\beta_{33}^{T}$, respectively. The strain components for both elastic and piezoelectric materials can be expressed by means of the displacement components ($u_r$ and $u_\theta$) as

$$\begin{cases} S_\theta = \dfrac{u_r}{r} + \dfrac{1}{r}\dfrac{\partial u_\theta}{\partial \theta} \\ S_r = \dfrac{\partial u_r}{\partial r} \\ S_{r\theta} = \dfrac{1}{r}\dfrac{\partial u_r}{\partial \theta} + \dfrac{\partial u_\theta}{\partial r} - \dfrac{u_\theta}{r} \end{cases} \tag{2a}$$

For piezoelectric materials, there is another set of geometrical equations between the electric field and the electrical potential $\phi$ as

$$\begin{cases} E_\theta = -\dfrac{1}{\mathrm{r}}\dfrac{\partial \phi}{\partial \theta} \\ E_r = -\dfrac{\partial \phi}{\partial r} \end{cases} \tag{2b}$$

On the other hand, without consideration of body force, the equilibrium equations for both elastic and piezoelectric materials are given by

$$\begin{cases} \dfrac{\partial T_r}{\partial r} + \dfrac{1}{r}\dfrac{\partial T_{r\theta}}{\partial \theta} + \dfrac{T_r - T_\theta}{r} = 0 \\ \dfrac{\partial T_{r\theta}}{\partial r} + \dfrac{1}{r}\dfrac{\partial T_\theta}{\partial \theta} + \dfrac{2T_{r\theta}}{r} = 0 \end{cases} \tag{3a}$$

Moreover, without consideration of body charge, the induction components in the piezoelectric materials should satisfy the following equilibrium equation

$$\frac{1}{r}\frac{\partial D_\theta}{\partial \theta} + \frac{D_r}{r} + \frac{\partial D_r}{\partial r} = 0 \tag{3b}$$

Besides, in order to ensure that displacement can be found by integrating the strain field, strains must satisfy the following compatibility equation

$$\left(\frac{\partial^2}{\partial r^2} + \frac{2}{r}\frac{\partial}{\partial r}\right) S_\theta + \left(\frac{1}{r^2}\frac{\partial^2}{\partial \theta^2} - \frac{1}{r}\frac{\partial}{\partial r}\right) S_r = \left(\frac{1}{r^2}\frac{\partial}{\partial \theta} + \frac{1}{r}\frac{\partial^2}{\partial r \partial \theta}\right) S_{r\theta} \tag{4}$$

Solutions of the above equations for the piezoelectric transducer under shearing stress, radial stress and electrical potential simultaneously will be discussed in the following sections.

## 3. Exact analysis for the piezoelectric transducer

### *3.1 General solution of the basic equations for piezoelectric layer*

The solution of the expansion transducer as shown in Fig. 1(a) can be found by correctly assembling the above solutions of the elastic layers and piezoelectric layer. The performance of the actuator is different before and after contact between the two elastic layers 2 and 3. So, the two cases should be considered separately as shown in Figs. 1(b) and 1(c), respectively.

#### *3.1.1 Case 1: Before contact*

For case 1, when the elastic layer 2 and 3 are not contacted, the transducer shown in Fig. 1(b) may suffer no shearing stress on the outer surface of the elastic layer 2. The expressions for the *i*-th elastic layer ($i = 1, 2, 3$) and the piezoelectric layer under the external potential are solved to be (see appendix for the detail procedure)

$$\begin{cases} T_{\theta Ei} = -C_{3Ei} S_E r^{-S_E-1} + C_{4Ei} S_E r^{S_E-1} \\ T_{rEi} = C_{3Ei} r^{-S_E-1} + C_{4Ei} r^{S_E-1} \\ T_{r\theta Ei} = 0 \end{cases} \quad \text{(for elastic layer 1, 2, 3, } i = 1, 2, 3) \tag{5a}$$

$$\begin{cases} T_{\theta P} = -C_{3P} S_P r^{-S_P-1} + C_{4P} S_P r^{S_P-1} \\ T_{rP} = C_{3P} r^{-S_P-1} + C_{4P} r^{S_P-1} - C_{5P} r^{-1} \\ E_r = -\dfrac{d\phi(r)}{dr}, \qquad D_r = \dfrac{S^D_{33P} C_{5P}}{g_{33} r} \\ E_\theta = 0, \qquad D_\theta = 0, \qquad T_{r\theta P} = 0 \end{cases} \quad \text{(for piezoelectric layer)} \tag{5b}$$

$$\begin{cases} u_{rEi} = e_1 C_{3Ei} r^{-S_E} + e_2 C_{4Ei} r^{S_E} \\ u_{\theta Ei} = 0 \end{cases} \quad \text{(for elastic layer 1, 2, 3)} \tag{6a}$$

$$\begin{cases} u_{rP} = p_1 C_{3P} r^{-S_P} + p_2 C_{4P} r^{S_P} + p_3 C_{5P} \\ u_{\theta P} = 0 \\ \phi = p_4 C_{3P} r^{-S_P} + p_5 C_{4P} r^{S_P} - p_6 C_{5P} \ln r + C_{0P} \end{cases} \quad \text{(for piezoelectric layer)} \tag{6b}$$

in which

$$S_E = \sqrt{\frac{S_{33E}}{S_{11E}}}, \qquad S_P = \sqrt{\frac{S^D_{33P}}{S^D_{11P}}} \tag{7}$$

$$\begin{cases} e_1 = S_{13E} - \dfrac{S_{33E}}{S_E}, \quad e_2 = S_{13E} + \dfrac{S_{33E}}{S_E} \\ p_1 = S^D_{13P} - \dfrac{S^D_{33P}}{S_P}, \quad p_2 = S^D_{13P} + \dfrac{S^D_{33P}}{S_P}, \quad p_3 = \dfrac{g_{31} S^D_{33P}}{g_{33}} - S^D_{13P} \\ p_4 = g_{31} - \dfrac{g_{33}}{S_P}, \quad p_5 = g_{31} + \dfrac{g_{33}}{S_P}, \quad p_6 = g_{33} + \dfrac{\beta^T_{33} S^D_{33P}}{g_{33}} \end{cases} \tag{8}$$

Where $C_{kEi}$ and $C_{kP}$, $C_{5P}$, $C_{0P}$ ($i = 1, 2, 3$; $k = 3, 4$) are constants of the $i$-th elastic layer and the piezoelectric layer, which can be determined by using geometrical and electrical boundary conditions.

The boundary conditions of stresses and displacements at the outer and inner surfaces satisfy the following three equations:

$$u_{rE1}\big|_{r=R_0} = 0 \tag{9}$$

$$\left.\frac{\partial u_{rE1}}{\partial \theta}\right|_{r=R_0} = 0 \tag{10}$$

$$T_{rE3}\big|_{r=R_3} = 0 \tag{11}$$

Here, Eq. (10) satisfies Eq. (6a) automatically. The other two equations can be expanded as

$$e_1 C_{3E1} R_0^{-S_E} + e_2 C_{4E1} R_0^{S_E} = 0 \tag{12}$$

$$C_{3E3} R_3^{-S_E-1} + C_{4E3} R_3^{S_E-1} = 0 \tag{13}$$

The boundary conditions for the electrical potentials ($\phi|_{r=R_1} = V_0$ and $\phi|_{r=R_2} = 0$) are equivalent to the following two equations, respectively

$$p_4 C_{3P} R_1^{-S_P} + p_5 C_{4P} R_1^{S_P} - p_6 C_{5P} \ln R_1 + C_{0P} = V_0 \tag{14}$$

$$p_4 C_{3P} R_2^{-S_P} + p_5 C_{4P} R_2^{S_P} - p_6 C_{5P} \ln R_2 + C_{0P} = 0 \tag{15}$$

Now consider the connecting conditions between any two adjacent layers, the mechanical continuous conditions at the interfaces ($T_{rP}\big|_{r=R_j} = T_{rEj}\big|_{r=R_j}$, $u_{rP}\big|_{r=R_j} = u_{rEj}\big|_{r=R_j}$, $j = 1, 2$) can be rewritten as

$$C_{3Ej} R_j^{-S_E-1} + C_{4Ej} R_j^{-S_E-1} = C_{3P} R_j^{-S_P-1} + C_{4P} R_j^{S_P-1} - C_{5P}/R_j \tag{16}$$

$$e_1 C_{3Ej} R_j^{-S_E} + e_2 C_{4Ej} R_j^{S_E} = p_1 C_{3P} R_j^{-S_P} + p_2 C_{4P} R_j^{S_P} + p_3 C_{5P} \tag{17}$$

The above independent Eqs. (12)-(17) can be used to determine the unknown constants $C_{kEi}$, $C_{kP}$, and $C_{5P}$ as well as $C_{7P}$ ($i = 1, 2$; $k = 3, 4$), which have the form

$$C_{4E2} = \frac{-V_0}{p_4(R_2^{-S_P} - R_1^{-S_P})\lambda_{3p} + p_5(R_2^{S_P} - R_1^{S_P})\lambda_{4p} - p_6 \ln(R_2/R_1)\lambda_{5p}} \tag{18}$$

$$\begin{cases} C_{3E1} = \lambda_{31} C_{4E2}, \quad C_{4E1} = \lambda_{41} C_{4E2} \\ C_{3E2} = \lambda_{32} C_{4E2} \\ C_{3P} = \lambda_{3P} C_{4E2}, \quad C_{4P} = \lambda_{4P} C_{4E2}, \quad C_{5P} = \lambda_{5P} C_{4E2} \\ C_{0P} = V_0 - p_4 C_{3P} R_1^{-S_P} - p_5 C_{4P} R_1^{S_P} + p_6 C_{5P} \ln R_1 \end{cases} \tag{19}$$

and the following notations are introduced

$$\begin{cases} \lambda_{31} = -\dfrac{e_2}{e_2} R_0^{2S_E} \lambda_{41}, \quad \lambda_{41} = \eta_{41}^1 \lambda_{3P} + \eta_{41}^2 \lambda_{4P}, \quad \lambda_{32} = R_3^{2S_E} \\ \lambda_{3P} = \dfrac{\gamma_1 a_4^2 - \gamma_2 a_4^1}{a_3^1 a_4^2 - a_3^2 a_4^1}, \quad \lambda_{4P} = \dfrac{\gamma_1 a_3^2 - \gamma_2 a_3^1}{a_3^2 a_4^1 - a_3^1 a_4^2} \\ \lambda_{5P} = R_2^{-S_P} \lambda_{3P} + R_2^{S_P} \lambda_{4P} - (R_2^{-S_E} \lambda_{32} + R_2^{S_E}) \end{cases} \tag{20}$$

$$\begin{cases} \gamma_1 = p_3(-R_3^{2S_E} R_2^{-S_E} + R_2^{S_E}) - e_1 R_3^{2S_E} R_2^{-S_E} + e_2 R_2^{S_E} \\ \gamma_2 = -R_3^{2S_E} R_2^{-S_E} + R_2^{S_E} \end{cases} \tag{21}$$

$$\begin{cases} a_3^1 = (p_1 + p_3) R_2^{-S_P}, \quad a_4^1 = (p_2 + p_3) R_2^{S_P} \\ a_3^2 = (-\dfrac{e_2}{e_1} R_0^{2S_P} R_1^{-S_E} + R_1^{S_E}) \eta_{41}^1 + R_2^{-S_P} - R_1^{-S_P} \\ a_4^2 = (-\dfrac{e_2}{e_1} R_0^{2S_P} R_1^{-S_E} + R_1^{S_E}) \eta_{41}^2 + R_2^{S_P} - R_1^{S_P} \end{cases} \tag{22}$$

$$\begin{cases} \eta_{41}^1 = \dfrac{(p_1 + p_3) R_1^{-S_P}}{(-e_2 p_3 / e_1) R_0^{2S_E} R_1^{-S_E} + p_3 R_1^{S_E} + e_2 (R_0^{2S_P} R_1^{-S_E} + R_1^{S_E})} \\ \eta_{41}^2 = \dfrac{(p_2 + p_3) R_1^{S_P}}{(-e_2 p_3 / e_1) R_0^{2S_E} R_1^{-S_E} + p_3 R_1^{S_E} + e_2 (R_0^{2S_P} R_1^{-S_E} + R_1^{S_E})} \end{cases} \tag{23}$$

Now, all the mechanical and electrical solutions of the transducer under the electrical potential on the surface of the piezoelectric layer have been obtained based on the theory of piezo-elasticity.

### *3.1.2 Case 2: After contact*

When the elastic layer 2 and 3 are contacted, the transducer shown in Fig. 1(c) may suffer the shearing stress and the radial stress on the outer surface of the elastic layer 3 and the electrical potential on the surface of the piezoelectric layer simultaneously. In the same manner as case 1, the expressions for the *i*-th elastic layer ($i$ = 1, 2, 3) and the piezoelectric layer are solved to be

$$\begin{cases} T_{\theta Ei} = -C_{3Ei} S_E r^{-S_E - 1} + C_{4Ei} S_E r^{S_E - 1} \\ T_{rEi} = C_{3Ei} r^{-S_E - 1} + C_{4Ei} r^{S_E - 1} \\ T_{r\theta Ei} = C_{6Ei} / r^2 \end{cases} \quad \text{(for elastic layer, } i\text{=1, 2, 3)} \tag{24a}$$

$$\begin{cases} T_{\theta P} = -C_{3P} S_P r^{-S_P - 1} + C_{4E} S_P r^{S_P - 1} \\ T_{rP} = C_{3P} r^{-S_P - 1} + C_{4P} r^{S_P - 1} - C_{5P} r^{-1} \\ E_r = -\dfrac{d\phi(r)}{dr}, \qquad D_r = \dfrac{S_{33P} C_{5P}}{g_{33} r} \\ E_\theta = 0, \qquad D_\theta = \dfrac{g_{15} C_{6P}}{\zeta_{11} r^2}, \qquad T_{r\theta P} = \dfrac{C_{6P}}{r^2} \end{cases} \quad \text{(for piezoelectric layer)} \tag{24b}$$

$$\begin{cases} u_{rEi} = e_1 C_{3Ei} r^{-S_E} + e_2 C_{4Ei} r^{S_E} \\ u_{\theta Ei} = r D_{3Ei} - \dfrac{S_{44E} C_{6Ei}}{2r} \end{cases} \quad \text{(for elastic layer, } i\text{=1, 2, 3)} \tag{25a}$$

$$\begin{cases} u_{rP} = p_1 C_{3P} r^{-S_P} + p_2 C_{4P} r^{S_P} + p_3 C_{5P} \\ u_{\theta P} = r D_{3P} - (S_{44P}^{D} + \dfrac{g_{15}^2}{\beta_{11}^{\mathrm{T}}}) \dfrac{C_{6P}}{2r} \\ \phi = p_4 C_{3P} r^{-S_P} + p_5 C_{4P} r^{S_P} - p_6 C_{5P} \ln r + C_{0P} \end{cases} \quad \text{(for piezoelectric layer)} \tag{25b}$$

where the subscript "*E*" and "*P*" in Eqs. (5) and (6) also denote the corresponding variables and constants in the elastic layers and piezoelectric layer, respectively. $C_{kEi}$, $C_{3Ei}$ and $C_{kP}$, $C_{3P}$, $C_{5P}$ as well as $C_{7P}$ ($i$ = 1, 2, 3; $k$ = 3, 4, 6) are constants of the $i$-th elastic layer and the piezoelectric layer, which can be determined by using geometrical and electrical boundary conditions.. And notations $e_1$-$e_2$, $p_1$-$p_6$ are same with Eq. (8).

Here, considering the elastic layer 2 is different from the elastic layer 3, the follow notations are used for the elastic layer 3

$$\begin{cases} e_1' = S_{13E}' - \dfrac{S_{33E}'}{S_E'} \\ e_2' = S_{13E}' + \dfrac{S_{33E}'}{S_E'} \\ S_E' = \sqrt{\dfrac{S_{33E}'}{S_{11E}'}} \end{cases} \tag{26}$$

where, $S_{11E}'$, $S_{13E}'$, $S_{33E}'$, $S_{44E}'$ are the elastic compliance for elastic layer 3.

The boundary conditions of the stresses and displacements at the outer and inner surfaces satisfy the following equations

$$u_{rE1}\big|_{r=R_0} = u_{\theta E1}\big|_{r=R_0} = 0 \tag{27}$$

$$\left.\frac{\partial u_{rE1}}{\partial \theta}\right|_{r=R_0} = 0 \tag{28}$$

$$T_{rE3}\big|_{r=R_5} = -\sigma_0 \tag{29}$$

$$T_{r\theta E3}\big|_{r=R_5} = \tau_0 \tag{30}$$

where, Eq. (28) satisfies automatically. The other three equations can be expanded as

$$e_1 C_{3E1} R_0^{-S_E} + e_2 C_{4E1} R_0^{S_E} = 0 \tag{31}$$

$$R_0 D_{3E1} - \frac{S_{44E} C_{6E1}}{2R_0} = 0 \tag{32}$$

$$C_{3E3} R_5^{-S_E'-1} + C_{4E3} R_5^{S_E'-1} = -\sigma_0 \tag{33}$$

$$C_{6E3}/R_5^2 = \tau_0 \tag{34}$$

The boundary conditions of the electrical potentials ($\phi\big|_{r=R_1} = V_0$ and $\phi\big|_{r=R_2} = 0$) are equivalent

to the following two equations, respectively

$$p_4 C_{3P} R_1^{-S_P} + p_5 C_{4P} R_1^{S_P} - p_6 C_{5P} \ln R_1 + C_{0P} = V_0 \tag{35}$$

$$p_4 C_{3P} R_2^{-S_P} + p_5 C_{4P} R_2^{S_P} - p_6 C_{5P} \ln R_2 + C_{0P} = 0 \tag{36}$$

Now considering the connecting conditions between any two adjacent layers, the mechanical continuous conditions at the interfaces ($T_{rP}\big|_{r=R_j} = T_{rEj}\big|_{r=R_j}$, $T_{r\vartheta P}\big|_{r=R_j} = T_{r\theta Ej}\big|_{r=R_j}$, $u_{rP}\big|_{r=R_j} = u_{rEj}\big|_{r=R_j}$, $u_{\theta P}\big|_{r=R_j} = u_{\theta Ej}\big|_{r=R_j}$, $T_{rE2}\big|_{r=R_4} = T_{rE3}\big|_{r=R_4}$, $T_{r\vartheta E2}\big|_{r=R_4} = T_{r\theta E3}\big|_{r=R_4}$, $u_{rE2}\big|_{r=R_3} - \delta = u_{rE3}\big|_{r=R_4}$, $u_{\theta E2}\big|_{r=R_4} = u_{\theta E3}\big|_{r=R_4}$, $j = 1,2$) can be rewritten as

$$C_{3Ej} R_j^{-S_E-1} + C_{4Ej} R_j^{-S_E-1} = C_{3P} R_j^{-S_P-1} + C_{4P} R_j^{S_P-1} - C_{5P}/R_j \tag{37}$$

$$C_{6Ej}/R_j^2 = C_{6P}/R_j^2 \tag{38}$$

$$e_1 C_{3Ej} R_j^{-S_E} + e_2 C_{4Ej} R_j^{S_E} = p_1 C_{3P} R_j^{-S_P} + p_2 C_{4P} R_j^{S_P} + p_3 C_{5P} \tag{39}$$

$$R_j D_{3Ej} - \frac{S_{44E} C_{6Ej}}{2R_j} = R_j D_{3P} - \left( S_{44P}^D + \frac{g_{15}^2}{\beta_{11}^T} \right) \frac{C_{6P}}{2R_j} \tag{40}$$

$$C_{3E2} R_4^{-S_E-1} + C_{4E2} R_4^{-S_E-1} = C_{3E3} R_4^{-S_E'-1} + c_{4E3} R_4^{-S_E'-1} \tag{41}$$

$$C_{6E2}/R_4^2 = C_{6E3}/R_4^2 \tag{42}$$

$$e_1 C_{3E2} R_3^{-S_E} + e_2 C_{4E2} R_3^{S_E} - \delta = e_1' C_{3E3} R_4^{-S_E'} + e_2' C_{4E3} R_4^{S_E'} \tag{43}$$

$$R_4 D_{3E2} - \frac{S_{44E} C_{6E2}}{2R_4} = R_4 D_{3E3} - \frac{S_{44E}' C_{6E3}}{2R_4} \tag{44}$$

The above independent Eqs. (31)-(44) can be used to determine the unknown constants $C_{kEi}$, $C_{kP}$, $D_{3Ei}$, $D_{3P}$ and $C_{5P}$ as well as $C_{7P}$ ($i$ = 1, 2, 3; $k$ = 3, 4, 6), which have the form

$$C_{4E3} = \frac{-V_0 - p_4 (R_2^{-S_P} - R_1^{-S_P}) \delta_{3p} - p_5 (R_2^{S_P} - R_1^{S_P}) \delta_{4p} + p_6 \ln(R_2/R_1) \delta_{5p}}{p_4 (R_2^{-S_P} - R_1^{-S_P}) \lambda_{3p} + p_5 (R_2^{S_P} - R_1^{S_P}) \lambda_{4p} - p_6 \ln(R_2/R_1) \lambda_{5p}} \tag{45}$$

$$\begin{cases} C_{3E1} = \lambda_{31} C_{4E3} + \delta_{31}, \quad C_{4E1} = \lambda_{41} C_{4E3} + \delta_{41} \\ C_{3E2} = \lambda_{32} C_{4E3} + \delta_{32}, \quad C_{4E2} = \lambda_{42} C_{4E3} + \delta_{42} \\ C_{3E3} = \lambda_{33} C_{4E3} + \delta_{33} \\ C_{3P} = \lambda_{3P} C_{4E3} + \delta_{3P}, \quad C_{4P} = \lambda_{4P} C_{4E3} + \delta_{4P}, \quad C_{5P} = \lambda_{5P} C_{4E3} + \delta_{5P} \\ C_{0P} = V_0 - p_4 C_{3P} R_1^{-S_P} - p_5 C_{4P} R_1^{S_P} + p_6 C_{5P} \ln R_1 \end{cases} \tag{46}$$

$$C_{6E1} = C_{6E2} = C_{6E3} = C_{6P} = \tau_0 R_5^2 \tag{47}$$

$$\begin{cases} D_{3E1} = \dfrac{S_{44E}\tau_0 R_5^2}{2R_0^2} \\ D_{3P} = D_{3E1} + (S_{44P}^D + \dfrac{g_{15}^2}{\beta_{11}^T} - S_{44E})\dfrac{\tau_0 R_5^2}{2R_1^2} \\ D_{3E2} = D_{3E3} = D_{3P} - (S_{44P}^D + \dfrac{g_{15}^2}{\beta_{11}^T} - S_{44E})\dfrac{\tau_0 R_5^2}{2R_2^2} \\ D_{3E3} = D_{3E2} - (S_{44E} - S'_{44E})\dfrac{\tau_0 R_5^2}{2R_2^2} \end{cases} \tag{48}$$

in which the following notations are introduced

$$\begin{cases} \lambda_{31} = -\dfrac{e_2}{e_2} R_0^{2S_E}\lambda_{41}, \quad \delta_{31} = -\dfrac{e_2}{e_2} R_0^{2S_E}\delta_{41}, \quad \lambda_{33} = -R_5^{2S'_E}, \quad \delta_{33} = -\sigma_0 R_5^{S'_E+1} \\ \lambda_{41} = \eta_{41}^1\lambda_{3P} + \eta_{41}^2\lambda_{4P}, \quad \delta_{41} = \eta_{41}^1\delta_{3P} + \eta_{41}^2\delta_{4P} \\ \lambda_{32} = \dfrac{(e'_2 R_4^{S'_E} - R_5^{2S'_E}R_4^{-S'_E}e'_1)R_4^{S_E} - (R_4^{S'_E} - R_5^{2S'_E}R_4^{-S'_E})R_3^{S_E}e_2}{R_3^{-S_E}R_4^{S_E}e_1 - R_3^{S_E}R_4^{-S_E}e_2}, \quad \delta_{32} = \dfrac{\delta R_4^{S_E} + R_4^{-S'_E}R_5^{S'_E+1}\sigma_0(R_3^{S_E}e_2 - R_4^{S_E}e'_1)}{R_3^{-S_E}R_4^{S_E}e_1 - R_3^{S_E}R_4^{-S_E}e_2} \\ \lambda_{42} = \dfrac{(e'_2 R_4^{S'_E} - R_5^{2S'_E}R_4^{-S'_E}e'_1)R_4^{-S_E} - (R_4^{S'_E} - R_5^{2S'_E}R_4^{-S'_E})R_3^{-S_E}e_1}{R_3^{S_E}R_4^{-S_E}e_2 - R_3^{-S_E}R_4^{S_E}e_1}, \quad \delta_{42} = \dfrac{\delta R_4^{-S_E} + R_4^{-S'_E}R_5^{S'_E+1}\sigma_0(R_3^{-S_E}e_1 - R_4^{-S_E}e'_1)}{R_3^{S_E}R_4^{-S_E}e_2 - R_3^{-S_E}R_4^{S_E}e_1} \end{cases} \tag{49}$$

$$\begin{cases} \lambda_{3P} = \dfrac{\gamma_1 a_4^2 - \gamma_2 a_4^1}{a_3^1 a_4^2 - a_3^2 a_4^1}, \quad \delta_{3P} = \dfrac{\eta_1 a_4^2 - \eta_2 a_4^1}{a_3^1 a_4^2 - a_3^2 a_4^1} \\ \lambda_{4P} = \dfrac{\gamma_1 a_3^2 - \gamma_2 a_3^1}{a_3^2 a_4^1 - a_3^1 a_4^2}, \quad \delta_{4P} = \dfrac{\eta_1 a_3^2 - \eta_2 a_3^1}{a_3^2 a_4^1 - a_3^1 a_4^2} \\ \lambda_{5P} = R_2^{-S_P}\lambda_{3P} + R_2^{S_P}\lambda_{4P} - (R_2^{-S_E}\lambda_{32} + R_2^{S_E}\lambda_{42}) \\ \delta_{5P} = R_2^{-S_P}\delta_{3P} + R_2^{S_P}\delta_{4P} - (R_2^{-S_E}\delta_{32} + R_2^{S_E}\delta_{42}) \end{cases} \tag{50}$$

$$\begin{cases} \gamma_1 = (e_1 + p_3)R_2^{-S_E}\lambda_{32} + (e_2 + p_3)R_2^{S_E}\lambda_{42} \\ \eta_1 = (e_1 + p_3)R_2^{-S_E}\delta_{32} + (e_2 + p_3)R_2^{S_E}\delta_{42} \\ \gamma_2 = R_2^{-S_E}\lambda_{32} + R_2^{S_E}\lambda_{42}, \quad \eta_2 = R_2^{-S_E}\delta_{32} + R_2^{S_E}\delta_{42} \\ a_3^1 = (p_1 + p_3)R_2^{-S_P}, \quad a_4^1 = (p_2 + p_3)R_2^{S_P} \\ a_3^2 = (-\dfrac{e_2}{e_1}R_0^{2S_P}R_1^{-S_E} + R_1^{S_E})\eta_{41}^1 + R_2^{-S_P} - R_1^{-S_P} \\ a_4^2 = (-\dfrac{e_2}{e_1}R_0^{2S_P}R_1^{-S_E} + R_1^{S_E})\eta_{41}^2 + R_2^{S_P} - R_1^{S_P} \end{cases} \tag{51}$$

$$\begin{cases} \eta_{41}^1 = \dfrac{(p_1 + p_3)R_1^{-S_P}}{-e_2(1 + p_3/e_1)R_0^{2S_P}R_1^{-S_E} + (e_2 + p_3)R_1^{S_E}} \\ \eta_{41}^2 = \dfrac{(p_2 + p_3)R_1^{S_P}}{-e_2(1 + p_3/e_1)R_0^{2S_P}R_1^{-S_E} + (e_2 + p_3)R_1^{S_E}} \end{cases} \tag{52}$$

Now, all the mechanical and electrical solutions of the transducer under shearing stress, radial stress and electrical potential simultaneously have been obtained based on the theory of piezo-

elasticity. From Eqs. (25), (47) and (48), it can be readily found that the displacement $u_\theta$ and the shear stress $T_{r\theta}$ in case 2 are not equal to zero and influenced only by the external shearing stress. In other words, the magnitude of the external shearing stress $\tau_0$ has no influence on the magnitude of the displacement $u_r$ and the normal stresses $T_r$, $T_\theta$.

## 4. Numerical results and comparisons

In the previous sections, the piezoelectric hollow cylinder transducer was theoretically analyzed, and the exact solutions were obtained. In order to compare the analytical solutions with the finite element results to verify the correctness of the analytical solutions, the following geometrical parameters are taken: $R_0$=0.08 m, $R_1$=0.01m, $R_2$=0.016 m, $R_3$=0.018 m, $R_4$=(0.018+$\delta$)m, $R_5$=0.024 m. The size of the gap is taken as $\delta = 2\times10^{-8}$ m unless otherwise mentioned. Besides, it is assumed that the piezoelectric layer is made of PZT-4, and its material parameters are listed in Table 1. The elastic layer 1 and 2 are made of aluminum; the elastic layer 2 is made of copper, and their material parameters as shown in Table 1 and Table 2. Moreover, the external radial stress $\sigma_0$ and the friction coefficient $\mu$ are taken as 100 KN/m$^2$ and 0.2, respectively.

Letting the gap between the two elastic layers be zero, the critical voltages $V_c$ are found to be 367.4 V in this transducer. When the applied voltage is below the critical value, case 1 as shown in Fig. 1(b) should be considered; otherwise, case 2 in Fig. 1(c) should be considered. The normal stresses ($T_r$, $T_\theta$), displacement $u_r$ and electrical potential $\phi$ are plotted versus the radius $r$ in Figs. 2-5. For this transducer, from Figs. 2-4, it can be found that the elastic layer 1 and 3 is compressed, while the elastic layer 2 is stretched, which will be discussed later in detail. Furthermore, the results of the finite element analysis by using Ansys 9.0 and 2D element (such as plane223 element for piezoelectric layer and plane42 element for elastic layers) are drawn in the Fig. 4 too. It can be found that the analytical solutions are consistent with the finite element results of Ansys, which verifies the correctness of the analytical solutions obtained in Section 3. Besides, it can be found that, after contact, the radial stress $T_r$ in the third elastic layer is almost same with the external radial stress $\sigma_0$, while the displacement $u_r$ has a mutation because of the gap $\delta$. Fig. 5 shows the electrical potential $\phi$ changes almost linearly in the radius direction in the piezoelectric layer under

Table 1 Material parameters of PZT-4 (for model-*g* constitutive relations)

| Elastic compliance ($10^{-12}$ m$^2$/N) | | | | Piezoelectric constant ($10^{-3}$ C/N) | | | Dielectric impermeability constant ($10^6$ m/F) | |
|---|---|---|---|---|---|---|---|---|
| $S_{11}^D$ | $S_{13}^D$ | $S_{33}^D$ | $S_{44}^D$ | $g_{31}$ | $g_{33}$ | $g_{15}$ | $\zeta_{11}(\beta_{11})$ | $\zeta_{33}(\beta_{33})$ |
| 7.95 | -3.03 | 7.91 | 17.91 | -17.77 | 23.91 | 40.36 | 76.87 | 99.65 |

Table 2 Material properties and thickness of the layers (for model A and model B)

| Layer | Material | Thickness (m) | Elastic modulus $E_i$ (GPa) | Poisson's ratio $v_i$ |
|---|---|---|---|---|
| 1 | Aluminum | 0.002 | 70 | 0.34 |
| Piezoelectric | PZT-4 | 0.006 | — | — |
| 2 | Aluminum | 0.002 | 70 | 0.34 |
| Gap($\delta$) | — | $2\times10^{-8}$ | — | — |
| 3 | Copper | 0.006 | 110 | 0.33 |

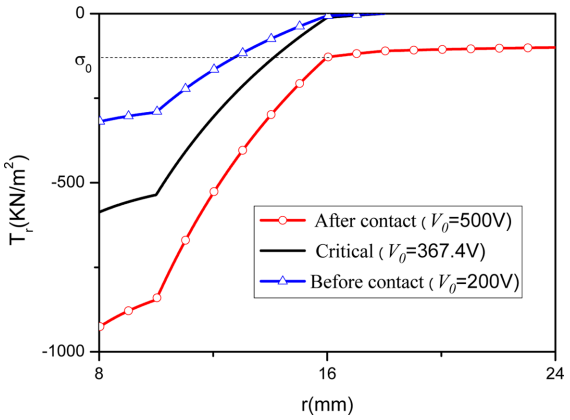


Fig. 2 The normal stress $T_r$ changing with the radius $r$

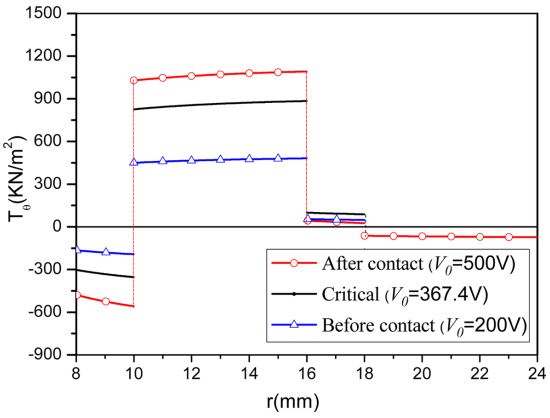


Fig. 3 The normal stress $T_\theta$ changing with the radius $r$

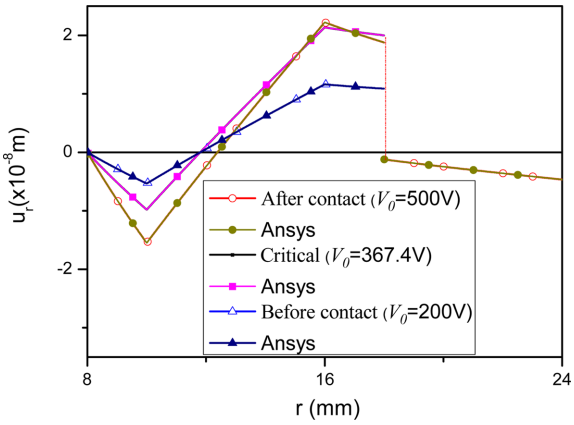


Fig. 4 The displacement $u_r$ changing with the radius $r$

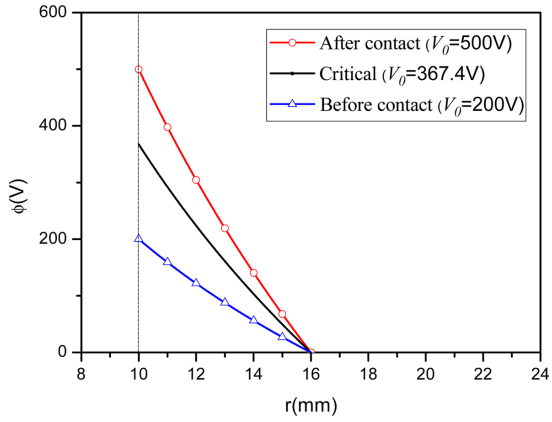


Fig. 5 The electrical potential $\phi$ changing with the radius $r$

the corresponding stress conditions. The displacement $u_\theta$ and the shearing stress $T_{r\theta}$ in case 2 are plotted versus the friction coefficient $\mu$ in Figs. 6 and 7, respectively. It is found that $T_{r\theta}$ decreases with $r$ and increases with the friction coefficient $\mu$, which means $T_{r\theta}$ decreases with $r$ and increases with the external shearing stress $\tau_0$; while the $u_\theta$ increases with $r$ and the external shearing stress $\tau_0$. Furthermore, Fig. 8 to Fig. 10 show the relationship between the normal stresses ($T_r$, $T_\theta$), displacement $u_r$ and the external radial stress $\sigma_0$ under the $\tau_0 = 100$ N/m, $V_0 = 500$ V. Figs. 8 and 9 denote the influence of the change of the external radial stress $\sigma_0$ for the normal stresses ($T_r$, $T_\theta$) is not proportional to the change of the external radial stress $\sigma_0$. From Fig. 10, it can be found the elastic layer 3 can be compressed or stretched with different value of $\sigma_0$. Moreover, in Figs. 11 and 12 $u_r$ at the interface ($r = R_3$) is plotted versus the applied voltage $V_0$ and the piezoelectric parameters $g_{33}$, respectively. It can be found that the $u_r$ at $r = R_3$ increases with the applied voltage $V_0$ and the increasing rate before contact is faster than that after contact. Besides, Fig, 12 shows that the piezoelectric parameters $g_{33}$ greatly influences the $u_r$; the larger the $g_{33}$, the larger the $u_r$. In other words, if one chooses the piezoelectric material with large $g_{33}$, the small critical voltage can be obtained for both actuators. Furthermore, Fig. 13 gives the relationship between the external radial

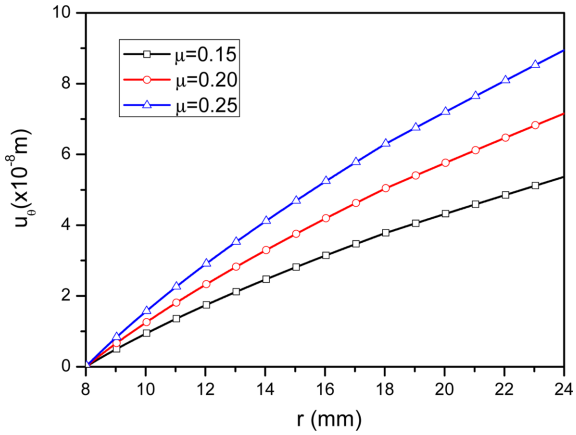


Fig. 6 The displacement $u_\theta$ changing with the radius $r$ after contact

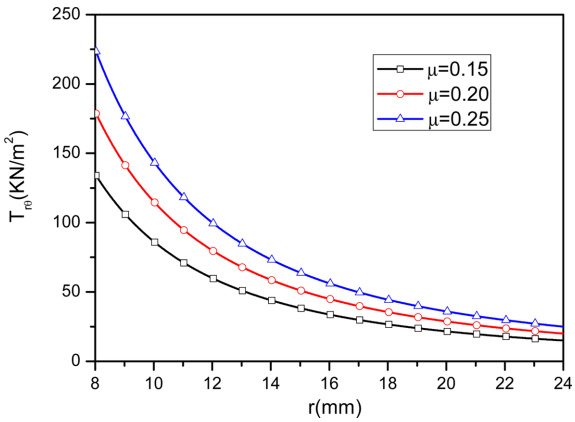


Fig. 7 The shear stress $T_{r\theta}$ changing with the radius $r$ after contact

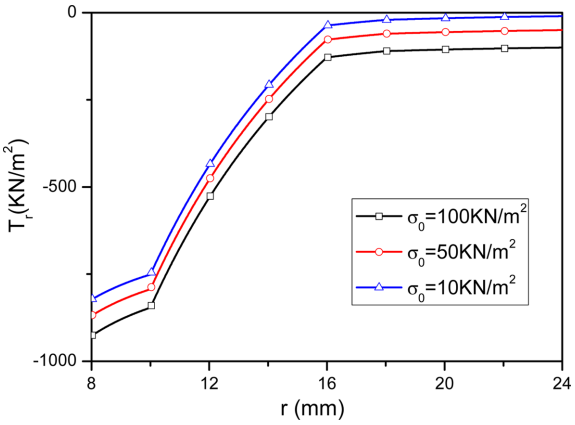


Fig. 8 The normal stress $T_r$ changing with the radius $r$ with different external radial stress $\sigma_0$

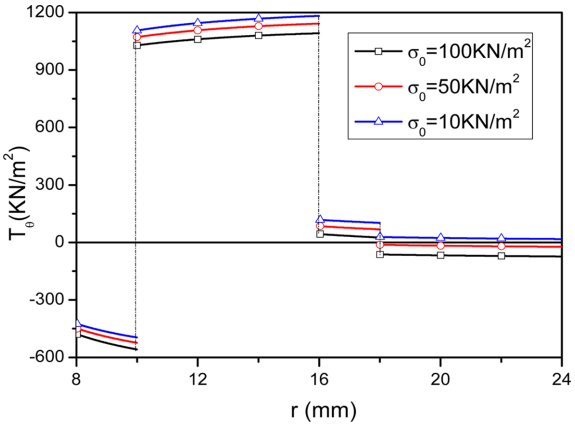


Fig. 9 The normal stress $T_\theta$ changing with the radius $r$ with different external radial stress $\sigma_0$

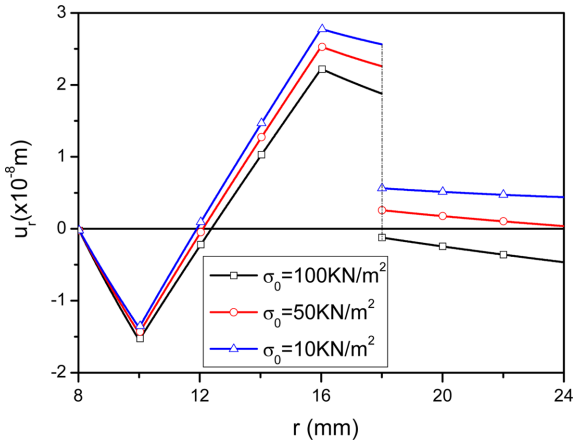


Fig. 10 The normal displacement $u_r$ changing with the radius $r$ with different external radial stress $\sigma_0$

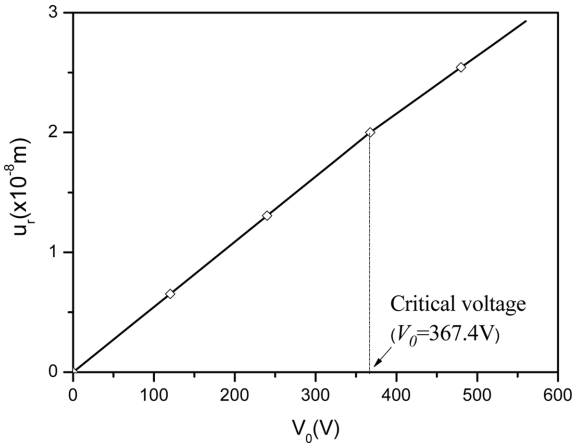


Fig. 11 The displacement $u_r$ at $r = R_3$ changing with the applied voltage $V_0$

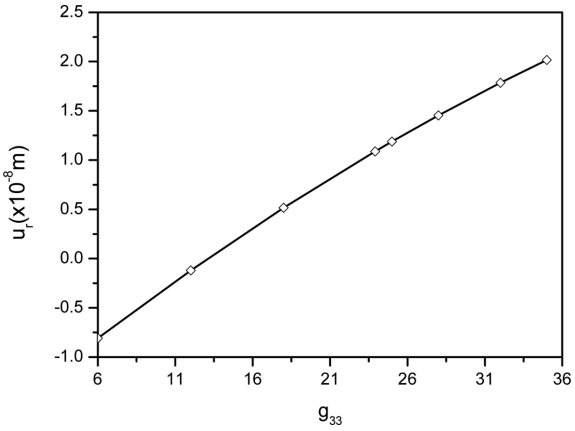


Fig. 12 The displacement $u_r$ at $r = R_3$ changing with the piezoelectric parameter $g_{33}$

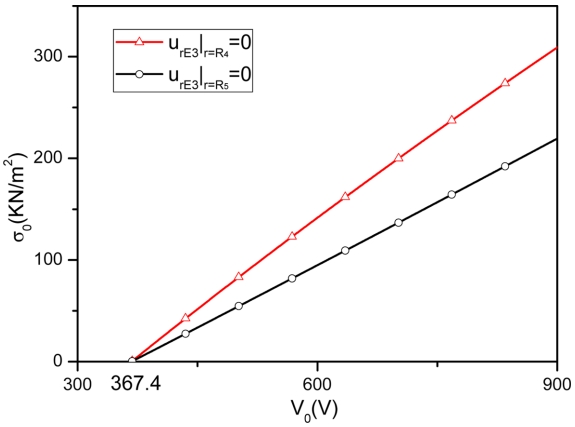


Fig. 13 The external radial stress $\sigma_0$ at $u_{rE3}\big|_{r=R_4}=0$ and $u_{rE3}\big|_{r=R_5}=0$ changing with the external potential $V_0$

stress $\sigma_0$ and the external potential $V_0$ considering $u_{rE3}\big|_{r=R_4} = 0$ and $u_{rE3}\big|_{r=R_5} = 0$ which mean the radial displacement $u_{rE3}$ of the target layer (elastic layer 3) keeps as zero on the inner and outer surface, respectively. It can be found the external radial stress $\sigma_0$ changes almost linearly with the external potential $V_0$ for this transducer.

## 5. Conclusions

An analytical study on the piezoelectric hollow cylinder transducer under shearing stress, radial stress and electrical potential simultaneously is presented based on the theory of piezo-elasticity. The exact solutions for this transducer are obtained by combining all the equations and boundary conditions, which is very helpful for the design of the bearing controllers. Moreover, the exact solutions can be used under plane strain or plane stress. The difference of the exact solutions under plane strain and plane stress reflects on the different values of the elastic coefficients $S_{klE}$ and $S_{klP}$. It is found that: 1) the elastic layer 3 can be compressed or stretched with different value of $\sigma_0$. 2) the external radial stress $\sigma_0$ changes almost linearly with the external potential $V_0$ for this transducer considering $u_{rE3}\big|_{r=R_4} = 0$ and $u_{rE3}\big|_{r=R_5} = 0$. 3) the displacement $u_\theta$ and the shear stress $T_{r\theta}$ in case 2 are not equal to zero and influenced only by the external shearing stress. 4) the magnitude of the external shearing stress $\tau_0$ has no influence on the magnitude of the displacement $u_r$ and the normal stresses $T_r$, $T_\theta$. 5). the extrusion stress $T_r$ increases with the increase of the piezoelectric parameter $g_{33}$ in the expansion actuator. 6). the external radial stress $\sigma_0$ changes almost linearly with the external potential $V_0$ for this transducer considering $u_{rE3}\big|_{r=R_4} = 0$ and $u_{rE3}\big|_{r=R_5} = 0$. 7). $T_{r\theta}$ decreases with $r$ and increases with the external shearing stress $\tau_0$; while the $u_\theta$ increases with $r$ and the external shearing stress $\tau_0$. 8). It is very helpful for the design of the bearing controllers.

## Acknowledgements

This work is supported by the National Natural Science Foundation of China (50908007 and 51072018).

Support is also supplied by and the Fundamental Research Funds for the Central Universities (300477).

## References

Aldraihem, O.J. and Khdeir, A.A. (2006), "Analytical solutions of antisymmetric angle-ply laminated plates with thickness-shear piezoelectric actuators", *Smart Mater. Struct*., **15**(2), 232-242.

Almajid, A., Taya, M. and Hudnut, S. (2001), "Analysis of out-of-plane displacement and stress field in a piezocomposite plate with functionally graded microstructure", *Int. J. Solids Struct*., **38**(19), 3377-3391.

Bboudi, J. (1991), *Mechanics of Composite Materials: a United Micromechanical Approach*, Amsterdam: Elsevier.

Chen, T.Y., Chung, C.T. and Lin, W.L. (2000), "A revisit of a cylindrically anisotropic tube subjected to pressuring, shearing, torsion, extension, and a uniform change", *Int. J. Solids Struct*., **37**(37), 5143-5159.

Chen, Y. and Shi, Z.F. (2005), "Exact solutions of functionally gradient piezothermoelastic cantilevers and parameter identification", *J. Intell. Mater. Syst. Struct*., **16**(6), 531-539.

Ding, H.J., Wang, H.M. and Chen, W.Q. (2003), "Analytical solution for the electroelastic dynamics of a nonhomogeneous spherically isotropic piezoelectric hollow sphere", *Arch. Appl. Mech*., **73**(1-2), 49-62.

Hagood, N.W. and Von, F.A. (1991), "Damping of structural vibrations with piezoelectric materials and passive electrical networks", *J. Sound Vib*., **146**(2), 243-268.

Han, R. and Shi, Z.F. (2008), "Exact analysis of two kinds of piezoelectric actuators", *Smart Mater. Struct*., **17**, 015018.

Hauke, T., Kouvatova, A., Steinhausena, R., Seiferta, W., Beigea, H., Theoa,H., Langhammera and Abichtb, H.P. (2000), "Bending behavior of functionally gradient materials", *Ferroelectrics*, **238**(1), 195-202.

Hou, P.F., Wang, H.M. and Ding, H.J. (2003), "Analytical solution for the axisymmetric plane strain electroelastic dynamics of a special non-homogeneous piezoelectric hollow cylinder", *Int. J. Eng. Sci*., **41**(16), 1849-1868.

Lee, S., Cho, B.C., Park, H.C., Yoon, K.J. and Goo, N.S. (2002), "Analysis of multi-layered actuators using an assumed strain solid element", *Mater. Chem. Phys*., **75**(1-3), 174-177.

Liu, Y.T. and Jiang, C.C. (2007), "Pneumatic actuating device with nanopositioning ability utilizing PZT impact force coupled with differential pressure", *Precis. Eng*., **37**(3), 293-303.

Liu, Y.T. and Higuchi, T. (2001), "Precision positioning device utilizing impact force of combined piezopneumatic actuator", *IEEE-ASME T. Mech*., **6**(4), 467-473.

Loewy, R.G. (1997), "Recent developments in smart structures with aeronautical applications", *Smart Mater. Struct*., **6**(5), R11-R42.

Mitchell, J.A. and Reddy, J.N. (1995), "A study of embedded piezoelectric layers in composite cylinders", *J. Appl. Mech.-T. ASME*., **62**(1) 166-173.

Muralt, P., Dohl, D.W. and Denk, W. (1986), "Wide-range, low-operating-voltage, bimorph stm: Application as potentiometer", *IBM J. Res. Dev*., **30**(5), 443-450.

Olesiak, Z.S. and Pyryev, Y.A. (1995), "A coupled quasi-stationary problem of thermodiffusion for an elastic cylinder", *Int. J. Eng. Sci*., **33**(6), 773-780.

Rao, S.S. and Sunar, M. (1994), "Piezoelectricity and its use in disturbance sensing and control of flexible structures: A survey", *Appl. Mech. Rev*. **47**(4), 113-123.

Sedighi, M.R. and Shakeri, M. (2009), "A three-dimensional elasticity solution of functionally graded piezoelectric cylindrical panels", *Smart Mater. Struct*., **18**.

Sharma, J.N., Pal, M. and Chand, D. (2004), "Three-dimensional vibration analysis of a piezothermoelastic cylindrical panel", *Int. J. Eng. Sci*., **42**(15-16), 1655-1673.

Shi, Z.F. (2005), "Bending behavior of piezoelectric curved actuator", *Smart Mater. Struct*., **14**(4), 835-842.

Shi, Z.F., Xiang, H.J. and Spencer, B.F. (2006), "Exact analysis of multi-layer piezoelectric/composite cantilevers", *Smart Mater. Struct*., **15**(5) 1447-1458.

Ting, T.C.T. (1999), "New solutions to pressuring, shearing, torsion and extension of a circular tube or bar", *Proc. R. Soc. Lond. A*., **455**(1989), 3527-3542.

Wang, Z.G., Abel, E.W., Millsb, R.P. and Liucm Y. (2002), "Assessment of multi-layer piezoelectric actuator technology for middleear implants", *Mechatronics*, **12**(1), 3-17.
Xiang, H.J., Shi, Z.F. and Zhang, T.T. (2006), "Elastic analyses of heterogeneous hollow cylinders", *Mech. Res. Commun*., **33**(5), 681-691.
Yoon, H.S. and Washington, G. (1998), "Piezoceramic actuated aperture antennae", *Smart Mater. Struct*., **7**(4), 537- 542.
Zhang, T.T. and Shi, Z.F. (2006), "Two-dimensional exact analysis for piezoelectric curved actuators", *J. Micromech. Microeng*., **16**(3) 640-647.
Zhang, T.T. and Shi, Z.F. (2007), "Bending behavior of 2-2 multi-layered piezoelectric curved actuators", *Smart Mater. Struct*., **16(3)**, 634-641.
Zhou, S.W., Liang, C. and Rogers, C.A. (1994), "Modeling of distributed piezoelectric actuators integrated with thin cylindrical-shells", *J. Acoust. Soc. Am*., **96**(3), 1605-1612.

*BS*

## Appendix

In the following equations, the variables $T$, $S$, $E$, $\phi$, $D$ and the unknown constants $C$ are same with those in Section 2 and 3; the subscript "$E$" and "$P$" also denote the corresponding variables and parameters in the elastic layers and piezoelectric layer, respectively.

### *A.1 before contact*

**For elastic layer *i* (*i*=1, 2, 3):**

Introducing *Airy* stress function $\Psi_{Ei}(r)$ for the elastic layer $i$, one has:

$$T_{rEi} = \frac{\Psi_{Ei}^{'}(r)}{r},\ T_{\theta Ei} = \Psi_{Ei}^{''}(r),\ T_{r\theta Ei} = 0 \tag{A1}$$

Using Eqs. (1a), (2a), (3a) and (4), *Airy* stress function $\Psi(r)$ can be obtained as follows

$$\Psi_{Ei}(r) = C_{1Ei} + C_{2Ei}r^2 + C_{3Ei}^{'}r^{(-S_E+1)} + C_{4Ei}^{'}r^{S_E+1} \tag{A2}$$

where $C_{jEi}$ ($j$ = 1~4) are undetermined constants. Based on the theory of elasticity, it can be easily understood that $C_{1Ei}$ needs not to be considered because it has no influence on the elastic field.

Substituting Eq. (A2) into Eq. (A1), the stress components can then be calculated by

$$\begin{cases} T_{\theta Ei} = \Psi''(r) = 2C_{2Ei} - C'_{3Ei}S_E(-S_E+1)r^{-S_E-1} + C'_{4Ei}S_E(S_E+1)r^{S_E-1} \\ T_{rEi} = \dfrac{\Psi'(r)}{r} = 2C_{2Ei} + C'_{3Ei}(-S_E+1)r^{-S_E-1} + C'_{4Ei}(S_E+1)r^{S_E-1} \end{cases} \tag{A3}$$

in which

$$S_E = \sqrt{\frac{S_{33}^E}{S_{11}^E}} \tag{A4}$$

Finally, the displacement and electrical potential components can be obtained by using Eqs. (2a) and (3a)

$$\begin{cases} u_{rEi} = S_{13}^E[2C_{2Ei}r + C'_{3Ei}(-S_E+1)r^{-S_E} + C'_{4Ei}(S_E+1)r^{S_E}] \\ \qquad + S_{33}^E[2C_{2Ei}r - C'_{3Ei}\dfrac{-S_E+1}{S_E}r^{-S_E} + C'_{4Ei}\dfrac{S_E+1}{S_E}r^{S_E}] + D_{1Ei}\cos\theta + D_{2Ei}\sin\theta \\ u_{\theta Ei} = 2C_{2Ei}(S_{11}^E - S_{33}^E)r\theta + D_{2Ei}\cos\theta - D_{1Ei}\sin\theta + rD_{3Ei} \end{cases} \tag{A5}$$

in which $D_{1Ei}$, $D_{2Ei}$, and $D_{3Ei}$ are constants to be determined.

Furthermore, the above equations can be simplified as follows according to the symmetrical characteristic and the boundary condition of the fixed end at the inner surface

$$\begin{cases} T_{\theta Ei} = -C_{3Ei}S_Er^{-S_E-1} + C_{4Ei}S_Er^{S_E-1} \\ T_{rEi} = C_{3Ei}r^{-S_E-1} + C_{4Ei}r^{S_E-1} \end{cases} \tag{A6}$$

$$\begin{cases} u_{rEi} = (S_{13}^E - \dfrac{S_{33}^E}{S_E})C_{3Ei}r^{-S_E} + (S_{13}^E + \dfrac{S_{33}^E}{S_E})C_{4Ei}r^{S_E} = e_1C_{3Ei}r^{-S_E} + e_2C_{4Ei}r^{S_E} \\ u_{\theta Ei} = 0 \end{cases} \tag{A7}$$

where

$$C_{3Ei} = C'_{3Ei}(-S_E+1),\ C_{4Ei} = C'_{4Ei}(S_E+1)$$

Eqs. (A6) and (A7) are same with Eqs. (5a) and (6a).

**For piezoelectric layer:**

Introducing *Airy* stress function $\Psi_P(r)$ for the piezoelectric layer is introduced and one has

$$T_{rP} = \frac{\Psi'_P(r)}{r},\ T_{\theta P} = \Psi''_P(r),\ T_{r\theta P} = 0 \tag{A8}$$

Furthermore, the electrical potential is assumed to be a function of the radius $r$ only, *i.e.* $\phi = \phi(r)$. Keeping the third expression in Eq. (A8) in mind, the following electrical field can be obtained from Eqs. (1b)-(3b):

$$E_\theta = 0,\ D_\theta = 0,\ E_r = \phi'(r),\ D_r = \frac{C_5}{r} \tag{A9}$$

where $C_5$ is a constant to be determined. Using Eqs. (1b)-(3b) and (4), *Airy* stress function $\Psi_P(r)$ can be obtained as follows:

$$\Psi_P(r) = C_{1P} + C_{2P}r^2 + C'_{3P}r^{(-S_P+1)} + C'_{4P}r^{S_P+1} - C_{5P}r \tag{A10}$$

where $C_i$ ($i$ = 1~4) are undetermined constants. Based on the theory of elasticity, it can be easily understood that $C_1$ needs not to be considered because it has no influence on the elastic field.

Substituting Eq. (A10) into Eq. (A8), the stress components can then be calculated by

$$\begin{cases} T_{\theta P} = \Psi_P''(r) = 2C_{2P} - C'_{3P}S_P(-S_P+1)r^{-S_P-1} + C'_{4P}S_P(S_P+1)r^{S_P-1} \\ T_{rP} = \dfrac{\Psi_P'(r)}{r} = 2C_{2P} + C'_{3P}(-S_P+1)r^{-S_P-1} + C'_{4P}(S_P+1)r^{S_P-1} - C_{5P}r^{-1} \end{cases} \tag{A11}$$

in which

$$S_P = \sqrt{\frac{S^D_{33}}{S^D_{11}}} \tag{A12}$$

Finally, the displacement and electrical potential components can be obtained by using Eqs. (2b) and (3b):

$$\begin{cases} u_{rP} = S^D_{13}[2C_{2P}r + C'_{3P}(-S_P+1)r^{-S_P} + C'_{4P}(S_P+1)r^{S_P}] + (\dfrac{g_{31}S^D_{33P}}{g_{33}} - S^D_{13P})C_{5P} \\ \qquad + S^D_{33}[2C_{2P}r - C'_{3P}\dfrac{-S_P+1}{S_P}r^{-S_P} + C'_4\dfrac{S_P+1}{S_P}r^{S_P}] + D_{1P}\cos\theta + D_{2P}\sin\theta \\ u_{\theta P} = 2C_{2P}(S^D_{11} - S^D_{33})r\theta + D_{2P}\cos\theta - D_{1P}\sin\theta + rD_{3P} \\ \phi = g_{31}[2C_{2P}r + C'_{3P}(-S_P+1)r^{-S_P} + C'_{4P}(S_P+1)r^{S_P}] - \beta^T_{33}\dfrac{S^D_{33P}}{g_{33}}C_{5P}\ln r + C_{0P} \\ \qquad + g_{33}[-C_{5P}\ln r + 2C_{2P}r - C'_{3P}\dfrac{-S_P+1}{S_P}r^{-S_P} + C'_{4P}\dfrac{S_P+1}{S_P}r^{S_P}] \end{cases} \tag{A13}$$

in which $D_{1P}$, $D_{2P}$, $D_{3P}$ and $C_6$ are constants to be determined.

Furthermore, for a piezoelectric hollow cylinder, the above equations can be simplified as follows according to the symmetrical characteristic

$$\begin{cases} T_{\theta P} = -C_{3P} S_P r^{-S_P-1} + C_{4E} S_P r^{S_P-1} \\ T_{rP} = C_{3P} r^{-S_P-1} + C_{4P} r^{S_P-1} - C_{5P} r^{-1} \\ E_r = -\dfrac{d\phi(r)}{dr}, \qquad D_r = \dfrac{S_{33P} C_{5P}}{g_{33} r} \\ E_\theta = 0, \qquad D_\theta = 0, \qquad T_{r\theta P} = 0 \end{cases} \tag{A14}$$

$$\begin{cases} u_{rP} = p_1 C_{3P} r^{-S_P} + p_2 C_{4P} r^{S_P} + p_3 C_{5P} \\ u_{\theta P} = 0 \\ \phi = p_4 C_{3P} r^{-S_P} + p_5 C_{4P} r^{S_P} - p_6 C_{5P} \ln r + C_{0P} \end{cases} \tag{A15}$$

where

$$C_{3P} = C'_{3P}(-S_P + 1),\ C_{4P} = C'_{4P}(S_P + 1)$$

$$\begin{cases} e_1 = S_{13E} - \dfrac{S_{33E}}{S_E}, \quad e_2 = S_{13E} + \dfrac{S_{33E}}{S_E} \\ p_1 = S^D_{13P} - \dfrac{S^D_{33P}}{S_P}, \quad p_2 = S^D_{13P} + \dfrac{S^D_{33P}}{S_P}, \quad p_3 = \dfrac{g_{31} S^D_{33P}}{g_{33}} - S^D_{13P} \\ p_4 = g_{31} - \dfrac{g_{33}}{S_P}, \quad p_5 = g_{31} + \dfrac{g_{33}}{S_P}, \quad p_6 = g_{33} + \dfrac{\beta^T_{33} S^D_{33P}}{g_{33}} \end{cases}$$

Eqs. (A14) and (A15) are same with Eqs. (5b) and (6b).

### *A.2 After contact*

**For elastic layer *i* (*i*=1, 2, 3):**

*Airy* stress function $\Psi_{Ei}(r, \theta)$ for the elastic layer $i$ can be obtained as follows

$$\Psi_{Ei}(r, \theta) = C_{1Ei} + C_{2Ei} r^2 + C'_{3Ei} r^{(-S_E+1)} + C'_{4Ei} r^{S_E+1} + C_{6Ei}\theta \tag{A16}$$

And one has

$$T_{rP} = \frac{\partial \Psi_E(r,\theta)}{r\partial r} + \frac{\partial^2 \Psi_E(r,\theta)}{r^2 \partial \theta^2}, \quad T_{\theta P} = \frac{\partial^2 \Psi_E(r,\theta)}{\partial r^2}, T_{r\theta P} = -\frac{\partial}{\partial r}\left(\frac{\partial \Psi_E(r,\theta)}{r\partial\theta}\right) \tag{A17}$$

**For piezoelectric layer:**

*Airy* stress function $\Psi_P(r, \theta)$ for the piezoelectric layer can be obtained as follows

$$\Psi_P(r, \theta) = C_{1P} + C_{2P} r^2 + C'_{3P} r^{(-S_P+1)} + C'_{4P} r^{S_P+1} - C_{5P} r + C_{6P}\theta \tag{A18}$$

And one has

$$T_{rP} = \frac{\partial \Psi_P(r,\theta)}{r\partial r} + \frac{\partial^2 \Psi_P(r,\theta)}{r^2 \partial \theta^2}, \quad T_{\theta P} = \frac{\partial^2 \Psi_P(r,\theta)}{\partial r^2}, T_{r\theta P} = -\frac{\partial}{\partial r}\left(\frac{\partial \Psi_P(r,\theta)}{r\partial\theta}\right) \tag{A19}$$

With the same procedure in above section, we can get the expressions in Eqs. (24) and (25).